

# Dating fluid infiltration using monazite

J.C. Ayers, M. Loflin & C.F. Miller  
*Vanderbilt University, Nashville, Tennessee, USA*

M.D. Barton  
*Univ. of Arizona, Tucson, Arizona, USA*

C. Coath  
*Dept. of Earth Sciences, Univ. of Bristol, Bristol, BS8 1RJ, United Kingdom*

**ABSTRACT:** Thermodynamic calculations at temperatures from 25-200°C and experimental measurements at 1.0 GPa and 1000°C show that the solubility of monazite (REEPO<sub>4</sub>) is low in near-neutral pH aqueous fluids but much higher in acidic and alkaline fluids. Acidic or alkaline fluids can recrystallize preexisting monazites or precipitate new monazites in contact metamorphic aureoles. Isotopic and geochronologic evidence from two aureoles suggests that monazite is more susceptible to hydrothermal alteration than zircon and may be used to map the extent and date the timing of fluid infiltration during contact metamorphism.

## 1 MONAZITE SOLUBILITY EXPERIMENTS

### 1.1 *Introduction and methods*

The solubility of monazite in pure H<sub>2</sub>O is low. At 25°C the concentration of Ce in a CePO<sub>4</sub>-saturated solution at pH = 7 is only  $\sim 10^{-14}$  molal. Even at 1.0 GPa and 1000°C the solubility is only  $\sim 0.007$  molal (Ayers 1991). At 25°C monazite solubility is known to increase as fluid acidity increases.

Because REE behave as hard acids, we would expect them to complex with hard acids, such as OH<sup>-</sup>, Cl<sup>-</sup> and F<sup>-</sup> (Langmuir 1997). Fitting equations of state to experimental data to estimate stability constants of REE complexes led Haas et al. (1995) to conclude that these would be the dominant ligands of REE, and that most dissolved REE would be complexed at elevated temperatures. We therefore conducted a series of experiments to characterize the effect of OH<sup>-</sup> and H<sup>+</sup> concentration on the solubility of monazite in order to identify compositions of fluids that could mobilize monazite.

Experimental measurement of the solubility of natural monazites in H<sub>2</sub>O ± HCl ± NaOH fluids used the single crystal mass loss method used previously by Ayers & Watson (1991, 1993). Cubes  $\sim 1$ -2 mm on edge were sawed from natural monazite crystals for use in solubility experiments. In terms of atoms per formula unit compositions ranges were Si 0.01-0.09, Th + U = 0.005-0.11, and Ca 0.002-0.025; Si and Th + U span the range of common monazite compositions, but Ca concentrations fall within the low end of that range. All experiments were conducted in a piston cylinder apparatus at 1.0 GPa and 1000°C. Cold-sealing capsules of the type described

by Ayers et al. (1992) were used to encapsulate samples. The solubility experiments were not designed for the extraction of thermodynamic data: pure end-member monazite compositions were not used, but as shown below, measurements using four different monazite compositions revealed no measurable difference in solubility, suggesting that the solubility of natural monazite does not depend strongly on its composition.

### 1.2 *Results and discussion*

Because we could not measure pH in-situ, we express pH relative to neutral at 25°C. This is equivalent to assuming that the added acid HCl or base NaOH completely dissociates at experimental conditions (the values of the dissociation constants of these salts at experimental conditions are unknown).

The amount of monazite dissolved in the fluid at run conditions is represented by the mass loss = initial crystal mass – final crystal mass. The mass of fluid = final mass of fluid + mass of dissolved monazite. The mass % solubility  $s = 100 * (\text{mass loss xt}) / (\text{mass loss xt} + \text{mass fluid})$ .

The time required to reach equilibrium was evaluated by conducting experiments of varying duration. Experiments run for 24 h and 48 h in pure H<sub>2</sub>O yield solubilities of 0.006 and 0.007 molal (assuming g.f.w of CePO<sub>4</sub>) that are the same within error. Solubilities measured in 2 m NaOH were 0.085 m at 12.4 h and 0.083 m at 24 h. Solubility in 0.1 m HCl was 0.002 m at 24 h and 0.001 m at 53 h. We conclude that 24 h and possibly just 12 h are required to reach equilibrium.

Measured solubilities appear to be independent of monazite composition within the range investigated (Fig. 1). In 2 m NaOH, measured solubilities were 0.083 m for Brazil monazite and 0.085 for Arendal monazite. In H<sub>2</sub>O, solubilities were 0.006 m and 0.007 m for Raade monazite and 0.005 m for Brazil monazite. In 0.01 m HCl, solubilities were 0.002 molal for EBay monazite and 0.001 m for Brazil monazite.

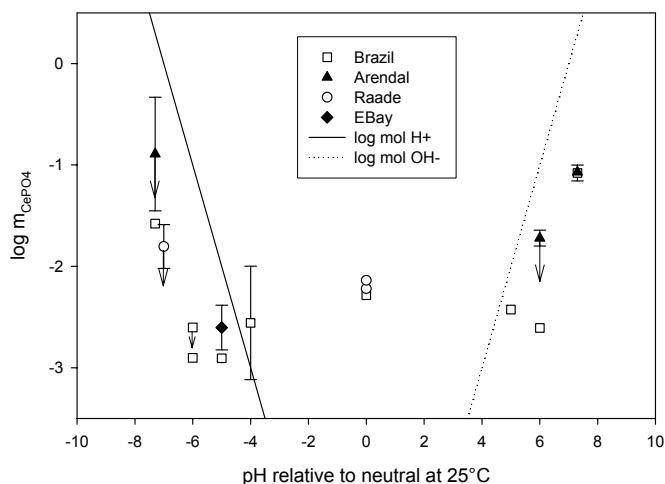


Figure 1. Measured aqueous solubility of monazite as a function of the concentration of H<sup>+</sup> in the initial fluid at 25°C. Concentrations of H<sup>+</sup> and OH<sup>-</sup> at 25°C are shown for comparison.

Measured solubilities demonstrate that the solubility of monazite at 1.0 GPa and 1000°C is very low, with  $m_{\text{REEPO}_4} < 0.01$  over a wide range of pH values. However, between pH = n-6 (neutral - 6 pH units) and n-7.3, the solubility increases by roughly two orders of magnitude from  $m_{\text{REEPO}_4} \sim 0.001$  to 0.1. Likewise, solubility is enhanced in strongly alkaline solutions, increasing from  $m_{\text{REEPO}_4} \sim 0.001$  to 0.1 when pH increases from pH = n+6 to n+7.3. This results in a U-shaped solubility curve characteristic of amphoteric solids. The solubility minimum occurs at near-neutral pH values where neutral complexes such as REE(OH)<sub>3</sub> predominate. At pH values < n-6 the activity of H<sup>+</sup> becomes high enough that it undergoes stepwise association with the hydroxyl ligands to form H<sub>2</sub>O: REE(OH)<sub>3</sub> + H<sup>+</sup> = REE(OH)<sub>2</sub><sup>+</sup> + H<sub>2</sub>O, and the ligand number decreases with decreasing pH until it equals zero and REE<sup>3+</sup> is the dominant species. At high pH values > n+6 the activity of OH<sup>-</sup> becomes high enough to form negatively charged complexes such as REE(OH)<sub>4</sub><sup>-</sup>. The formation of charged complexes enhances the solubility of monazite at low and high pH values because their concentrations are added to the constant (pH-independent) concentration of the neutral complex REE(OH)<sub>3</sub>. This type of pH-dependence of the solubility of REE compounds was demonstrated recently for Nd(OH)<sub>3(xt)</sub> (Wood et al. 2002).

Neutral complexes are favored when the dielectric constant of water  $\epsilon_{\text{H}_2\text{O}}$  is low. A very rough extrapolation suggests that  $\epsilon_{\text{H}_2\text{O}} \sim 10$  at the conditions of this study compared with a value of  $\sim 80$  at ambient conditions. This may explain the inference from the shape of the solubility curve that REE(OH)<sub>3</sub><sup>0</sup> predominate to 6 pH units below neutrality. However, an alternative explanation is that the range of pH values experimentally investigated does not extend over 12 orders of magnitude because the added salts did not completely dissociate at the experimental conditions. Just as it favors formation of neutral REE hydroxide complexes, a low value of  $\epsilon_{\text{H}_2\text{O}}$  inhibits dissociation of HCl and NaOH, i.e. HCl may behave as a weak acid and NaOH as a weak base at experimental conditions. Experimentally measured values of electrical conductance of dilute HCl-bearing solutions allowed (Frantz & Marshall 1984) to estimate the value of the dissociation constant of HCl from 100-700°C and pressures up to 4000 bars; using the equation fit to their experimental data and a density of 0.792 g/cm<sup>3</sup> estimated from the EOS of (Kerrick & Jacobs 1981) yields  $\log K_{\text{HCl}} = -3.87$ . This results in calculated pH values (Table 2) ranging from 3.53 at  $m_{\text{HCl}} = 0.001$  to 1.79 for  $m_{\text{HCl}} = 2$ . Plotting the data using these estimated pH values shows that the solubility remains constant, and by implication REE(OH)<sub>3</sub><sup>0</sup> remain the dominant species, until pH drops below 2. Unfortunately no data on the dissociation constant of NaOH at elevated pressures and temperatures are available. We conclude that significant amounts of monazite may dissolve and precipitate in the presence of acidic and alkaline fluids.

## 2 STUDIES OF MONAZITE IN CONTACT METAMORPHIC AUREOLES

### 2.1 Introduction and methods

We chose the contact metamorphic aureoles of two granitic plutons to investigate how monazite responds to infiltration of fluids in which it is soluble. Both aureoles contain monazite and display evidence of alteration by acidic magmatic fluids (sericitization). Contact metamorphism occurred at conditions under which monazite in granitic systems has been shown to be susceptible to hydrothermal alteration (Poitrasson et al. 2000): mildly acidic (and for Birch Creek oxidizing and saline) fluids at temperatures of  $\sim 250$ -400°C and pressures of  $\sim 0.15$ -0.4 GPa.

Monazites were separated from rock samples using standard methods, then mounted in epoxy and polished. The Cameca IMS 1270 Multi-Collector High Resolution Ion Microprobe at UCLA was used for in-situ analysis of zircon U-Pb ages and monazite  $\delta^{18}\text{O}$  and Th-Pb ages using backscattered electron images to guide our choice of analysis spots.

For geochronology, spots on individual grains were analyzed using standard procedures outlined in Quidelleur et al. (1997) and Miller et al. (2000).

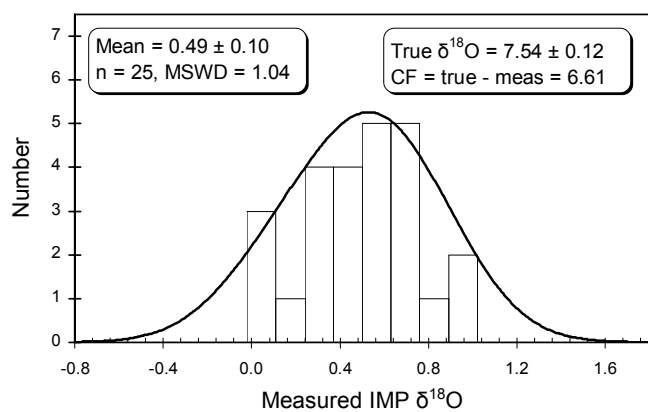


Figure 2. Histogram of  $\delta^{18}\text{O}$  values measured on standard 554 during one ion microprobe session. Mean values given with 95% confidence limits.

Most monazite and zircon analyses were corrected using  $^{204}\text{Pb}$ . Reported zircon ages are  $^{206}\text{Pb}/^{238}\text{U}$  for concordant and  $^{207}\text{Pb}/^{206}\text{Pb}$  for discordant zircons. For oxygen isotope analysis a  $\text{Cs}^+$  beam was used to sputter the sample and  $^{18}\text{O}^-$  and  $^{16}\text{O}^-$  beams collected simultaneously in two Faraday cups (Fayek et al. 2002). Analytical precision was typically 0.2 ‰ or better. Conventional mass spectrometric oxygen isotope analysis of monazite standards was performed by Bruce Taylor of the Geological Survey of Canada using a fluorination procedure followed by conventional gas source mass spectrometric analysis.

We used the measured conventional values for monazite standards  $\delta^{18}\text{O}$  Brazil = 1.43 ‰ and 554 = 7.54 ‰ as the “true” values to calculate the average values of correction factor  $\text{CF} = (\text{true} - \text{measured})$  for each of our two IMP sessions. In a given session standards 554 and Brazil have nearly identical correction factors even though their respective  $\text{ThO}_2$  concentrations of  $\sim 3.7\%$  and  $\sim 6.8\%$  are very different, suggesting that composition does not affect the value of  $\delta^{18}\text{O}$  measured on the IMP. Over two sessions the average of the standard deviation for multiple analyses of 554 was 0.46 ‰ (Fig. 2).

## 2.2 Results and discussion

Monazites from Ireteba are most intensely altered near the contact with the Searchlight pluton, but nearly all monazites contain altered secondary zones and unaltered primary zones, resulting in a bimodal Th-Pb age distribution with age ranges of 14-18 and 60-65 Ma corresponding to intrusion of the subjacent Searchlight pluton and primary crystallization of the Ireteba pluton (Townsend et al. 2000). In contrast, primary and secondary zones show no significant difference in corrected  $\delta^{18}\text{O}$  values (Fig. 3). If

fluids caused the monazite to partially recrystallize they did not significantly change the oxygen isotope compositions of the secondary zones, suggesting that fluids were in equilibrium with respect to oxygen isotope exchange. Monazites from the Ireteba pluton display two generations of monazite with very different ages and compositions, but identical  $\delta^{18}\text{O}$  distributions. This would occur if the fluid/rock ratio was low so that the oxygen isotope composition of the fluid was buffered by the rock, consistent with the low degree of hydrothermal alteration in the Ireteba pluton. In this situation altered zones date the timing of fluid infiltration, but oxygen isotopes do not fingerprint the fluid source because the  $\delta^{18}\text{O}$  of the infiltrating fluid was buffered by rock.

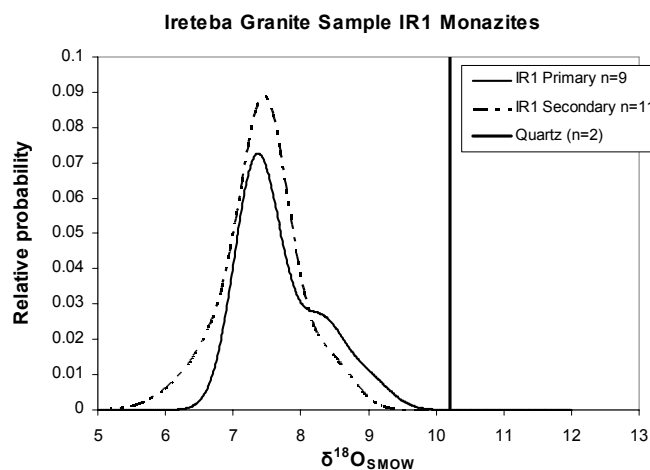


Figure 3. Cumulative histograms of corrected  $\delta^{18}\text{O}$  values of primary and secondary zones in monazites from sample IR1 measured on the IMP. Values for quartz from the same sample measured by conventional methods shown for comparison.

The Birch Creek pluton is a two-mica granite in the White Mountains of eastern California (Barton 2000). Monazites from the pluton show concentric euhedral magmatic zoning, mean  $\delta^{18}\text{O} = 8.2 \pm 0.2$  ‰ (Fig. 4) and mean Th-Pb age of  $78.0 \pm 0.7$  Ma ( $n = 28$ ). Monazites in the early Cambrian Deep Springs quartzite  $\sim 0.3$  km from the contact display patchy chaotic zoning but have similar ages ( $78.3 \pm 1.6$  Ma,  $n = 17$ ) and  $\delta^{18}\text{O}$  values ( $9.0 \pm 0.5$  ‰), and  $\sim 1$  km from the contact show concentric zoning,  $\delta^{18}\text{O} = 5.5 \pm 0.3$  ‰ and detrital ages (with some possibly low due to Pb loss) from 583-1069 Ma. Figure 5 shows the distinct difference in age and oxygen isotope compositions of altered monazites close to the contact, unaltered monazites far from the contact, and of three monazites close to the contact that plot as mixtures of altered and unaltered monazite. Monazites close to the contact completely recrystallized or were newly precipitated during fluid infiltration, while monazites  $\geq 1.0$  km away were unaffected. In contrast, zircons in the host rocks did not recrystallize, but preserved their magmatic zoning and Cambrian-Precambrian U-Pb ages.

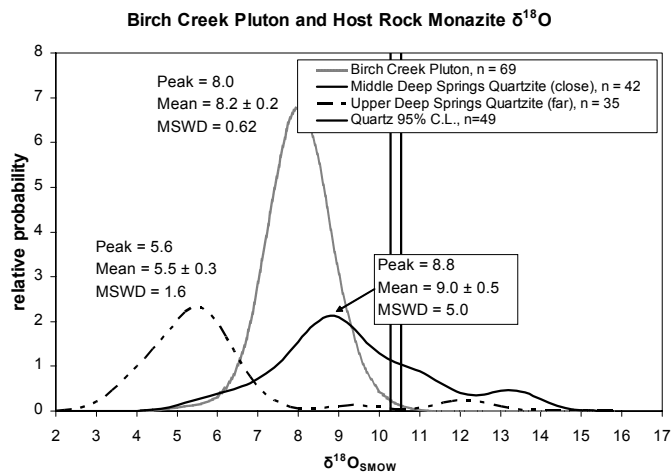


Figure 4. Cumulative histograms of corrected  $\delta^{18}\text{O}$  values measured using the IMP. 95% confidence limits on the mean value for quartz from the same units measured using conventional methods (Barton, unpub. data) shown for comparison.

Zircon is most reliable for dating events prior to hydrothermal activity, whereas monazite, being more susceptible to alteration by acidic or alkaline fluids, is useful for mapping the extent and timing of fluid infiltration events.

## REFERENCES

- Ayers, J. C. & Watson, E.B. 1991. Solubility of apatite, monazite, zircon and rutile in supercritical aqueous fluids with implications for subduction zone geochemistry. *Phil. Trans. Roy. Soc. Lond. A* 335: 365-375.
- Ayers, J. C., Brenan, J. B., Watson, E. B., Wark, D. A. & Minarik, W. G. 1992. A new capsule technique for hydrothermal experiments using the piston cylinder apparatus. *Amer. Min.* 77: 1080-1086.
- Ayers, J. C. & Watson, E. B. 1993. Rutile solubility and mobility in supercritical aqueous fluids: *Contrib. Mineral. Petrol.* 114: 321-330.
- Barton, M. D. 2000. Overview of the lithophile element-bearing magmatic-hydrothermal system at Birch Creek, White Mountains, CA; Field trip day one, Birch Creek, White Mountains, CA. In *SEG Guidebook Series* 32: 9-44.
- Fayek, M., Harrison, T. M., Ewing, R. C., Grove, M. & Coath, C. D. 2002. O and Pb isotopic analyses of uranium minerals by ion microprobe and U-Pb ages from the Cigar Lake deposit. *Chemical Geology* 185(3-4): 205-225.
- Frantz, J. D. & Marshall, W. L. 1984. Electrical conductances and ionization constants of salts, acids, and bases in supercritical aqueous fluids: I. Hydrochloric acid from 100° to 700°C and at pressures to 4000 bars. *American Journal of Science* 284: 651-667.
- Haas, J. R., Shock, E. L. & Sassani, D. C. 1995. Rare earth elements in hydrothermal systems: Estimates of standard partial molal thermodynamic properties of aqueous complexes of the rare earth elements at high pressures and temperatures. *Geochimica et Cosmochimica Acta* 59: 4329-4350.
- Kerrick, D. M. & Jacobs, G. K. 1981. A modified Redlich-Kwong equation for  $\text{H}_2\text{O}$ ,  $\text{CO}_2$ , and  $\text{H}_2\text{O}-\text{CO}_2$  mixtures at elevated pressures and temperatures. *American Journal of Science* 281: 735-767.

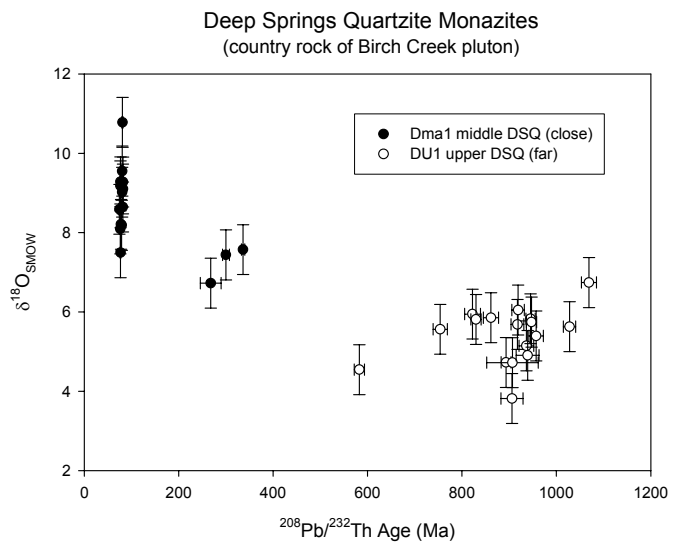


Figure 5. Distinct differences in Th-Pb ages and oxygen isotope compositions for monazites from the Deep Springs Quartzite ~0.3 km (close) and ~1 km (far) from the contact with the Birch Creek pluton.

- Langmuir D. 1997. *Aqueous Environmental Geochemistry*. Prentice Hall.
- Miller, C. F., Hatcher, R. D., Jr., Ayers, J. C., Coath, C. D. & Harrison, T. M. 2000. Age and zircon inheritance of eastern Blue Ridge plutons, southwestern North Carolina and northeastern Georgia, with implications for magma history and evolution of the Southern Appalachian Orogen. *American Journal of Science* 300: 142-172.
- Poitrasson, F., Chenery, S. & Shepherd, T.J. 2000. Electron microprobe and LA-ICP-MS study of monazite hydrothermal alteration: Implications for U-Th-Pb geochronology and nuclear ceramics. *Geochim. Cosmochim. Acta* 64: 3283-3297.
- Quidelleur, X., Grove, M., Lovera, O. M., Harrison, T. M., Yin, A. & Ryerson, F. J. 1997. Thermal evolution and slip history of the Renbu Zedong thrust, southeastern Tibet. *Jour. Geophys. Res.* 102: 2659-2679.
- Townsend, K. J., Miller, C. F., D'Andrea, J. L., Ayers, J. C., Harrison, T. M. & Coath, C. D. 2000. Low temperature replacement of monazite in the Ireteba granite, Southern Nevada: geochronological implications. *Chem. Geol.* 172: 95-112.
- Wood, S. A., Palmer D. A., Wesolowski D. J. & Benezeth P. 2002. The aqueous geochemistry of the rare earth elements and yttrium. Part XI. The solubility of  $\text{Nd}(\text{OH})_3$  and hydrolysis of  $\text{Nd}^{3+}$  from 30 to 290C at saturated water vapor pressure with in-situ pH measurement. In R. Hellmann & S. Wood (eds.), *Water-Rock Interactions, Ore Deposits, and Environmental Geochemistry: A Tribute to David A. Crerar, Special Publication 7*: 229-256. The Geochemical Society.